

Desmocollin-2 promotes intestinal mucosal repair by controlling integrin-dependent cell adhesion and migration

Sven Flemming^{a,†}, Anny-Claude Luissint^{a,†}, Dennis H. M. Kusters^a, Arturo Raya-Sandino^a, Shuling Fan^a, Dennis W. Zhou^b, Mizuho Hasegawa^a, Vicky Garcia-Hernandez^a, Andrés J. García^{b,c}, Charles A. Parkos^a, and Asma Nusrat^{a,*}

^aDepartment of Pathology, University of Michigan, Ann Arbor, MI 48109; ^bGeorge W. Woodruff School of Mechanical Engineering and ^cParker H. Petit Institute for Bioengineering and Biosciences, Georgia Institute of Technology, Atlanta, GA 30332

ABSTRACT The intestinal mucosa is lined by a single layer of epithelial cells that forms a tight barrier, separating luminal antigens and microbes from underlying tissue compartments. Mucosal damage results in a compromised epithelial barrier that can lead to excessive immune responses as observed in inflammatory bowel disease. Efficient wound repair is critical to reestablish the mucosal barrier and homeostasis. Intestinal epithelial cells (IEC) exclusively express the desmosomal cadherins, Desmoglein-2 and Desmocollin-2 (Dsc2) that contribute to mucosal homeostasis by strengthening intercellular adhesion between cells. Despite this important property, specific contributions of desmosomal cadherins to intestinal mucosal repair after injury remain poorly investigated *in vivo*. Here we show that mice with inducible conditional knockdown (KD) of Dsc2 in IEC (*Villin-Cre^{ERT2}; Dsc2^{fl/fl}*) exhibited impaired mucosal repair after biopsy-induced colonic wounding and recovery from dextran sulfate sodium-induced colitis. *In vitro* analyses using human intestinal cell lines after KD of Dsc2 revealed delayed epithelial cell migration and repair after scratch-wound healing assay that was associated with reduced cell–matrix traction forces, decreased levels of integrin β 1 and β 4, and altered activity of the small GTPase Rap1. Taken together, these results demonstrate that epithelial Dsc2 is a key contributor to intestinal mucosal wound healing *in vivo*.

Monitoring Editor

Keith Mostov
University of California,
San Francisco

Received: Dec 11, 2019

Revised: Jan 15, 2020

Accepted: Jan 17, 2020

INTRODUCTION

The intestinal epithelial barrier is created by a series of intercellular transmembrane adhesion and cytosolic protein complexes that form the apical junctional complex (AJC) consisting of the tight junction (TJ) and the adherens junction (AJ) (Farquhar and Palade, 1963; Laukoetter *et al.*, 2006). Additionally, spot-like adhesions or desmosomes (DMs) residing subjacent to the AJC, contribute to

controlling intercellular adhesion strength and epithelial homeostasis. The extracellular adhesive core in DMs is formed by the desmosomal cadherins desmoglein (Dsg) and Desmocollin (Dsc), which are single-pass transmembrane glycoproteins of the cadherin superfamily and calcium-dependent anchoring junctions. Four Dsg and three Dsc isoforms (Dsg 1–4 and Dsc 1–3) are expressed in a

This article was published online ahead of print in MBoc in Press (<http://www.molbiolcell.org/cgi/doi/10.1091/mbc.E19-12-0692>) on January 22, 2020.

[†]These authors contributed equally to this work.

Author contributions: S.F., A.-C.L., and D.K. designed and performed experiments, analyzed and interpreted data; S.F. and A.-C.L. wrote and revised the manuscript; A.R.-S., S.F., D.W.Z., M.H., and V.G.-H. assisted with collecting data; A.N. supervised the study, designed experiments, provided resources, wrote and edited the manuscript; A.J.G. and C.A.P. helped with design of experiments, provided resources, and edited the manuscript.

The authors declare no competing interests.

*Address correspondence to: Asma Nusrat (anusrat@umich.edu).

Abbreviations used: AJ, adherens junction; AJC, apical junctional complex; BSA, bovine serum albumin; CD, Crohn's disease; DAL, disease activity index; DAPI, 4',6'-diamidino-2-phenylindole, dihydrochloride; DM, desmosomes; Dsc,

desmocollin; Dsc2^{ERT2}, *Villin-Cre^{ERT2}*; Dsg, desmoglein; DSS, dextran sulfate sodium; EPAC, GEF protein directly activated by cAMP; GEF, guanine exchange factor; H&E, hematoxylin-eosin; IBD, inflammatory bowel disease; IEC, intestinal epithelial cells; IF, immunofluorescence; i.p., intraperitoneal; JAM-A, junctional adhesion molecule-A; KD, knockdown; mPAD, microfabricated post array detector; PBS, phosphate-buffered saline; Pkp3, Plakophilin-3; qPCR, quantitative PCR; Rap1, Ras-related protein 1; shRNA, short hairpin RNA; TBS, Tris-buffered saline; TJ, tight junction; UC, ulcerative colitis; WB, immunoblot analysis.

© 2020 Flemming, Luissint, *et al.* This article is distributed by The American Society for Cell Biology under license from the author(s). Two months after publication it is available to the public under an Attribution–Noncommercial–Share Alike 3.0 Unported Creative Commons License (<http://creativecommons.org/licenses/by-nc-sa/3.0/>).

“ASCB®,” “The American Society for Cell Biology®,” and “Molecular Biology of the Cell®” are registered trademarks of The American Society for Cell Biology.

tissue-specific and differentiation-specific manner. DM cadherins engage in a homo- or heterophilic manner and are internally linked to intermediate filament cytoskeleton through specific desmosomal plaque proteins including plakoglobin, plakophilins, and desmoplakin (Holthofer et al., 2007; Nekrasova and Green, 2013). DMs are highly enriched in tissues that experience extensive mechanical stress, such as cardiac muscle and epidermis as well as in the intestinal mucosa. Abnormal desmosomal function or disruption of desmosomal assembly causes several human pathologies comprising autoimmune diseases pemphigus vulgaris and pemphigus foliaceus, cardiomyopathy, epidermal and mucosal blistering, and cancer progression (Chidgey and Dawson, 2007; Waschke, 2008; Brooke, Nitoiu, and Kelsell, 2012; Huber and Petersen, 2015; Najor, 2018).

Epithelial barrier properties are critical in maintaining intestinal mucosal homeostasis, and a breach in this barrier results in pathological states that are associated with excessive exposure to microbial antigens, recruitment of leukocytes, release of soluble mediators, and ultimately mucosal damage seen in inflammatory bowel diseases (IBD). IBD pathogenesis that encompasses Crohn's disease (CD) and ulcerative colitis (UC), two main forms of chronic relapsing intestinal inflammation, is not well understood (Baumgart and Sandborn, 2012; Ordas et al., 2012). However, there is growing evidence that compromised intestinal barrier function plays a critical role in the epithelial damage and perpetuation of mucosal inflammation (inflammatory flares) by the recruitment of leukocytes into the subepithelial space that creates a local milieu enriched in soluble pro- and anti-inflammatory mediators that modulate epithelial barrier function (Gassler et al., 2001; Bruewer et al., 2006; Neurath, 2014). Furthermore, mucosal wound healing that is achieved by collective epithelial cell migration and proliferation is important to restore the epithelial barrier and suppress inflammatory responses (Neurath and Travis, 2012; Papi and Aratari, 2014; Brazil, Quiros, et al., 2019; Quiros and Nusrat, 2019).

Of note, intestinal epithelial cells (IEC) exclusively express Dsg2 and Dsc2 that have distinct binding properties and function in desmosome organization and adhesion. Dsc2 is reported to form homophilic bonds and heterophilic interactions with Dsg2, whereas Dsg2 engages only in heterophilic interactions (Schafer et al., 1994; Nuber et al., 1995; Syed et al., 2002; Lowndes et al., 2014). Dsc2 has been reported to play a major role in initiating desmosome assembly, whereas Dsg2 stabilizes the desmosomal complex (Roberts et al., 1998; Burdett and Sullivan, 2002; Lowndes et al., 2014). While Dsg2 has been reported to contribute to the intestinal epithelial barrier function, the role of DM cadherins in orchestrating in vivo repair of simple epithelia such as the intestinal epithelium remains undefined. Using predominantly in vitro models, we and others have observed that Dsg2 regulates intestinal epithelial proliferation and apoptosis (Nava, Laukoetter, et al., 2007; Schlegel et al., 2010; Ungewiss et al., 2017; Yulis, Quiros, et al., 2018). Conversely, the contributions of Dsc2 in controlling these cellular functions of simple epithelia remains less well understood. Loss of Dsc2 has been reported to promote IEC proliferation and colorectal cancer development (Funakoshi et al., 2008; Kolegraff et al., 2011). Interestingly, the expression of both, Dsg2 and Dsc2 is reduced in patients with CD, suggesting a role for Dsg2 and Dsc2 in the pathogenesis of inflammatory diseases in the intestine (Spindler et al., 2015; Gross et al., 2018). Recently, it has been reported that stable IEC-specific Dsg2 knockdown (KD) driven by the *Villin* promoter resulted in increased intestinal permeability in vivo and enhanced sensitivity to dextran sulfate sodium (DSS) as well as *Citrobacter rodentium*-induced colitis (Gross et al., 2018). Surprisingly, IEC-specific KD of

Dsc2 showed a lack of notable phenotype on intestinal epithelial barrier function in vivo and did not alter susceptibility to DSS-induced intestinal injury compared with control mice (Gross et al., 2018). These findings do not correlate with in vitro studies suggesting a major role for Dsc2 in desmosome biology (Roberts et al., 1998; Burdett and Sullivan, 2002; Lowndes et al., 2014).

To determine the role of Dsc2 in orchestrating intestinal mucosal repair after injury in vivo, we generated mice that harbor tamoxifen-inducible conditional KD of Dsc2 in IEC (*Villin-Cre^{ERT2}; Dsc2^{fl/fl}*, or *Dsc2^{ERT2/IEC}*). In this model, Dsc2 is acutely deleted in the adult mouse intestine, thereby serving as a model to analyze its role in epithelial repair. We describe the effect of KD of Dsc2 in two distinct models of epithelial injury and repair, namely, DSS-induced epithelial injury followed by a recovery period by discontinuation of DSS administration and colonic mucosal biopsy-induced wounds. Mechanistic analysis of the contribution of Dsc2 in intestinal epithelial repair after injury was conducted in vitro using human IEC lines. Herein we report that Dsc2 regulates intestinal mucosal wound closure by controlling cell–matrix adhesion dynamics and IEC migration.

RESULTS AND DISCUSSION

Targeted deletion of Dsc2 in IEC does not influence baseline intestinal mucosal architecture

To explore the contribution of Dsc2 in IEC biology and mucosal repair after injury, we generated *Dsc2^{ERT2/IEC}* mice that express an ERT2-Cre fusion protein under control of *Villin* promoter (el Marjou et al., 2004). Tamoxifen treatment resulted in acute selective deletion of Dsc2 in IEC that was confirmed in the colon from *Dsc2^{ERT2/IEC}* versus *Dsc2^{fl/fl}* control littermate mice by immunofluorescence (IF) labeling and Western blot analyses 30 d after tamoxifen administration (Figure 1, A and B). Consistent with a previous report, we found that acute loss of Dsc2 on IEC in vivo did not alter the protein levels of either Dsg2 or E-cadherin (Figure 1B) (Gross et al., 2018). Furthermore, histologic analysis of colonic mucosa in *Dsc2^{ERT2/IEC}* mice 30 d after tamoxifen treatment revealed no signs of colitis. The mucosa had normal architecture with no gross abnormalities or signs of immune cell infiltration and was indistinguishable from littermate controls (Figure 1, C and D). These results suggested that selective loss of Dsc2 on IEC does not grossly alter intestinal mucosal homeostasis.

Down-regulation of Dsc2 in human UC individuals and mouse colitis

It has been reported that patients with CD have altered ultrastructure of DMs by electron microscopy and have reduced expression of intestinal epithelial Dsg2 and Dsc2 (Spindler et al., 2015). In one study, decreased expression of colonic Dsc2 was observed in individuals with UC (Gassler et al., 2001). Therefore, we evaluated expression of Dsc2 in the intestinal mucosa of individuals with UC by IF labeling and immunoblotting and found that Dsc2 protein was decreased in mucosal tissue of individuals with active UC compared with mucosa without active disease (Figure 2, A and B). Similarly, expression of Dsc2 was reduced in the inflamed colon of mice with DSS-induced mucosal injury (Figure 2, C and D). Interestingly, we also detected reduced expression of low molecular weight cleavage fragments of Dsc2 in inflamed colon from individual with active UC and murine colitis.

Of note, studies from our laboratory and others have demonstrated the existence of proteolytic cleavage fragments of human Dsg2 caused by matrix metalloproteinases, caspases, and a disintegrin and metalloproteinase (ADAM) (Nava, Laukoetter, et al., 2007; Cirillo et al., 2008; Kolegraff et al., 2011). Proinflammatory cytokines

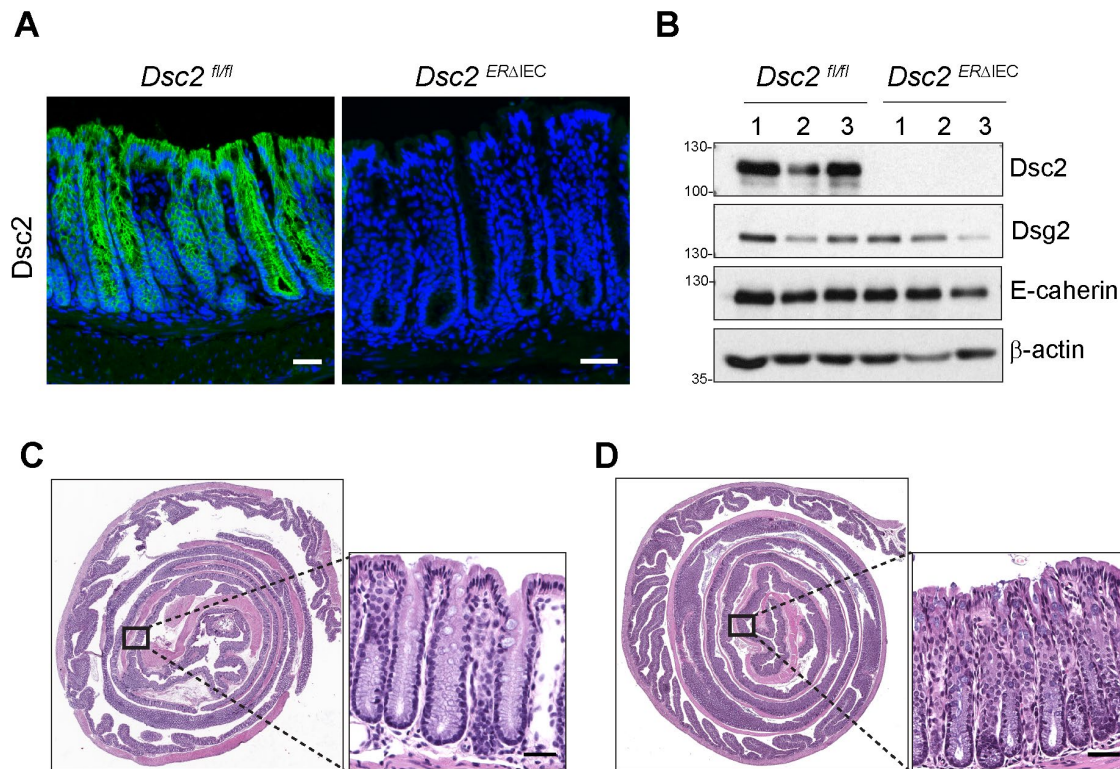


FIGURE 1: Selective loss of Dsc2 in IEC does not cause intestinal inflammation at baseline. *Dsc2^{ERAIEC}* mice were treated with tamoxifen to induce acute deletion of Dsc2 in IEC and analyzed 4 wk after the last tamoxifen injection. (A) Representative images of colon tissue stained with anti-Dsc2 antibodies (green) and DAPI (nuclei/blue). Dsc2 expression is absent in the colonic epithelium in *Dsc2^{ERAIEC}* mice compared with control *Dsc2^{fl/fl}* mice. Scale bars: 50 μ m. (B) Whole colonic tissue was homogenized, proteins were separated by SDS-PAGE, and PVDF membrane was immunoblotted for Dsc2, Dsg2, E-cadherin, and β -actin. Numbers 1–3 represent individual mice. (C, D) Representative images of H&E staining of section of Swiss roll mounts of the entire colon showing the gross mucosal architecture of *Dsc2^{ERAIEC}* vs. *Dsc2^{fl/fl}* mice. No signs of alteration of the epithelial barrier nor intestinal inflammation in *Dsc2^{ERAIEC}* (D) in comparison to control mice (C). Scale bars: 200 μ m.

such as interferon-gamma (IFN- γ) and tumor necrosis factor-alpha (TNF- α) released into the epithelial milieu during mucosal inflammation result in increased cleavage fragments of Dsg2 and ectodomain shedding from IEC in the intestinal mucosa from patients with active UC and in the mucosa of mice with DSS-induced colitis. These fragments have biological effects on cellular processes including proliferative signaling in epithelial cells, cell adhesion, and apoptosis (Schlegel *et al.*, 2010; Nava, Kamekura, and Nusrat, 2013; Kamekura *et al.*, 2015; Yulis, Quiros, *et al.*, 2018).

Interestingly, here we show that unlike Dsg2, the decrease in full-length Dsc2 protein did not appear to be related to accumulation of its proteolytic cleavage fragments in the intestinal mucosa of individuals with UC and in murine colitis. Furthermore, given that numerous reports have described that proinflammatory cytokines result in down-regulation of intercellular junction proteins of TJ, AJ, and DMs, it is tempting to speculate that proinflammatory mediators may control the expression of Dsc2 in IEC via distinct mechanisms compared with those that control Dsg2 (Luissint *et al.*, 2016). Further studies are needed to determine the molecular mechanisms involved in the down-regulation of Dsc2 expression.

Delayed recovery from acute colitis in mice with Dsc2 KD in IEC

We further examined the physiological role(s) of Dsc2 in mucosal responses to acute injury and repair using a murine model employing acute DSS-induced mucosal injury followed by recovery.

Dsc2^{ERAIEC} mice and *Dsc2^{fl/fl}* littermate controls were treated with DSS in drinking water for 5 d followed by a recovery period without DSS in water to evaluate mucosal recovery. During the recovery period, *Dsc2^{ERAIEC}* mice exhibited an exacerbated increased body weight loss compared with control mice (Figure 2E). Mice with >20% of body weight loss were killed and quantified in the Kaplan Meier survival curves (Supplemental Figure S1A). Eighty percent of *Dsc2^{fl/fl}* control mice survived in the course of the experiment and recovered from DSS-induced injury at day 10 in comparison to 44.5% of *Dsc2^{ERAIEC}* mice. These observations revealed that selective loss of Dsc2 on IEC resulted in increased morbidity and mortality during recovery from DSS colitis. Analysis of disease activity index (DAI), representing a score incorporating weight loss, stool consistency (diarrhea), and blood in stools similarly demonstrated poor recovery in *Dsc2^{ERAIEC}* mice compared with controls (Figure 2F). The elevated DAI scores also paralleled enhanced colon shortening after DSS, further supporting other parameters of mucosal inflammation in *Dsc2^{ERAIEC}* mice (Supplemental Figure S1B). Histological analysis of colonic mucosa 5 d after recovery from colitis revealed significantly worse mucosal injury in *Dsc2^{ERAIEC}* mice. Mucosal ulceration (crypt loss) was confined to the distal colon in *Dsc2^{fl/fl}* control mice, while *Dsc2^{ERAIEC}* mice had extensive ulcers that extended into the mid colon (Figure 2, G and H).

The above findings are at odds with a recent report that used constitutive deficient *Villin-Cre; Dsc2^{fl/fl}* and observed no consequences of loss of Dsc2 on IEC in the progression of DSS-induced

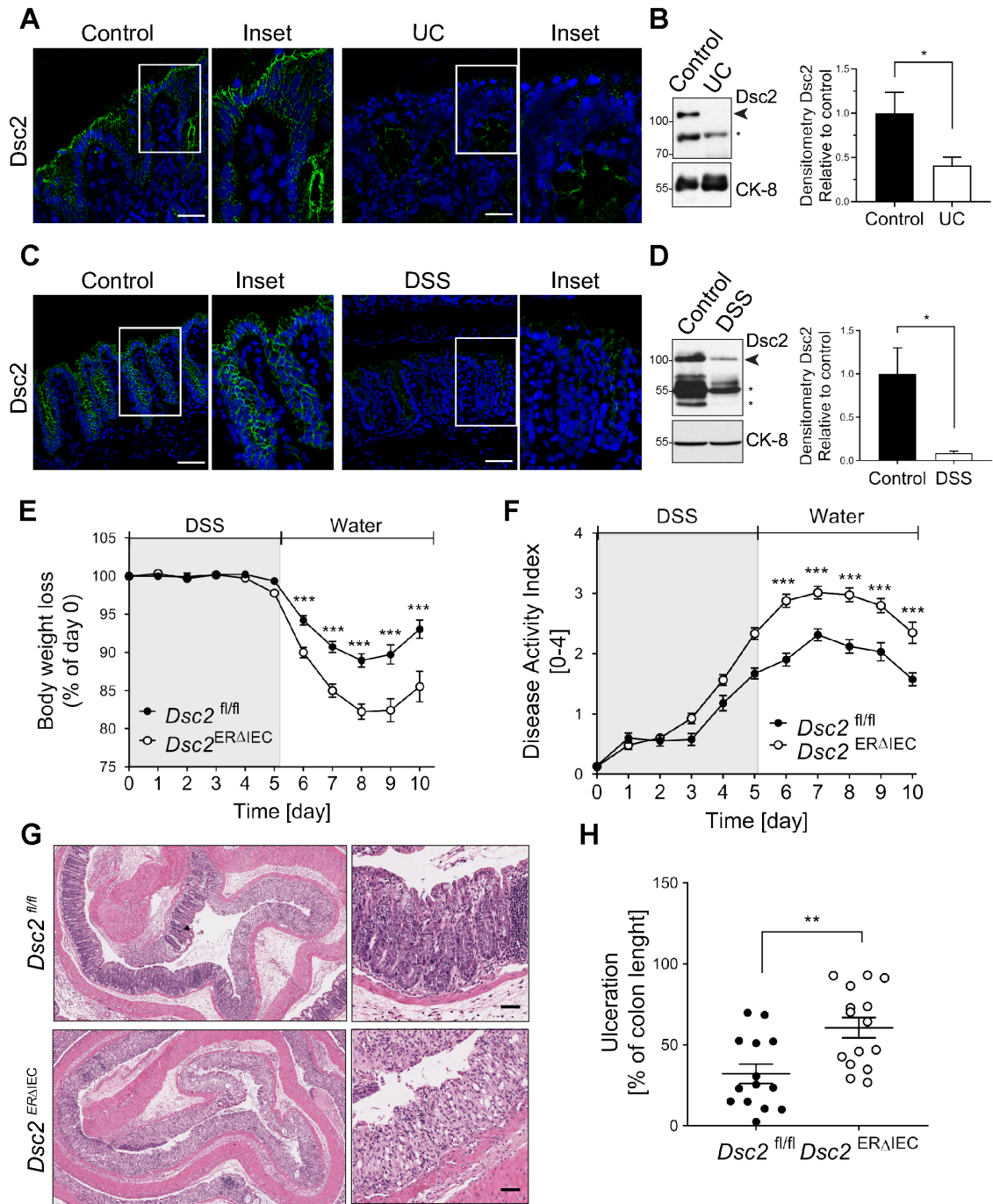


FIGURE 2: Dsc2 is decreased in human and mouse inflamed colon, and its loss resulted in delayed mucosal recovery from colitis. (A) Representative images of IF staining of Dsc2 (green) and DAPI (blue) in frozen sections of human colonic tissues from patients with UC and healthy controls. Reduction of fluorescence intensity for Dsc2 in UC compared with control. Scale bars: 50 μ m. (B) Western blot (WB) and densitometry analysis of the expression of Dsc2 and loading control Cytokeratin-8 (CK-8) in human colonic tissues from patients with UC and healthy controls. WB images are representative of two individual experiments with 10 controls and nine UC samples. Arrowhead: Full-length Dsc2; asterisk: cleaved Dsc2. Bar graphs represent densitometric values of seven healthy controls and six UC samples and are normalized to control. Data are mean \pm SEM. Significance is determined by two-tailed Student's *t* test. **p* \leq 0.05. (C, D) Reduced expression of Dsc2 in inflamed colonic mucosa from DSS-treated wild-type C57BL/6 mice at day 7 of DSS treatment (5 d DSS followed by 2 d of water) by IF and WB. (C) Representative IF images of frozen sections of colon tissue from DSS-treated mice vs. untreated controls. Dsc2 (green) and DAPI (blue). Reduction of fluorescence intensity for Dsc2 in DSS compared with control. Scale bars: 50 μ m. (D) Representative WB images and densitometry analysis of the expression of Dsc2 and CK-8 in colon from DSS-treated mice vs. untreated controls. Arrowhead: Full-length Dsc2; asterisk: cleaved Dsc2. Bar graphs represent values of three individual mouse per group and normalized to controls. Data are mean \pm SEM. Significance is determined by two-tailed Student's *t* test. **p* = 0.04. (E–H) Age- and sex-matched *Dsc2*^{ERΔIEC} and littermate control (*Dsc2*^{fl/fl}) mice were used 4 wk after the last tamoxifen

colitis in comparison to control mice (Gross *et al.*, 2018). Herein, a major difference is that we used animals with acute deletion of Dsc2 in IEC in adult mice that diminishes compensatory responses with other cadherins that have been reported for the loss of Dsg2 that resulted in up-regulation of Dsc2 *in vivo* and *in vitro* (Kamekura, Kolegraff, *et al.*, 2014; Gross *et al.*, 2018). Furthermore, in their experimental model, Gross *et al.* reported that loss of Dsc2 resulted in upregulation of Dsg-2-binding protein Galectin-3 in Dsc2-deficient mice (Gross *et al.*, 2018). In this study, Galectin-3 was suggested to compensate for the Dsc2 loss in IEC and account for the lack of phenotype seen in the intestinal mucosa Dsc2-deficient mice. We have previously reported that Galectin-3 associates with the ectodomain of Dsg-2 and stabilizes Dsg-2 at the cell surface leading to enhanced intercellular adhesion (Jiang, Rankin, *et al.*, 2014).

Taken together, our results show that acute loss of intestinal epithelial Dsc2 resulted in impaired epithelial recovery from DSS-induced injury indicating a protective role of Dsc2 in intestinal mucosal repair.

Delayed colonic mucosal wound healing after Dsc2 loss

To further examine the contribution of Dsc2 in intestinal mucosal repair, a second model of injury and repair was utilized that employs miniaturized endoscopic biopsy-induced wounds in the distal colon. Wound closure was quantified by digital imaging of the same wounds. Dsc2^{ERAIEC} mice exhibited significantly reduced wound repair 3 d after biopsy-induced injury compared with Dsc2^{fl/fl} controls supporting a role of Dsc2 in intestinal mucosal repair (Figure 3, A and B). IF labeling of epithelial E-cadherin in frozen sections of healing wounds was used to identify wound associated epithelial cells. Whereas the wound-associated epithelium was observed to cover wound beds in the Dsc2^{fl/fl} colonic mucosa, the Dsc2^{ERAIEC} colon wound bed was exposed with few E-cadherin expressing wound-associated epithelial cells covering denuded surfaces. These findings support impaired epithelial wound repair in the absence of IEC Dsc2 (Figure 3C).

Since efficient epithelial wound healing requires cell proliferation as well as coordinated collective migration of cells, we examined the effect of Dsc2 loss on IEC proliferation *in vivo* after biopsy-induced injury. Proliferation of epithelial cells adjoining the wound bed was evaluated by IF labeling of the well-accepted cell proliferation marker Ki67. Cell proliferation in crypts adjacent to the wound bed was not compromised after KD of Dsc2 in IEC (Figure 3D), suggesting that delayed wound closure after Dsc2 KD was not due to impaired epithelial cell proliferation. Altogether, our results suggest that the impaired repair is likely due to defective epithelial cell migration.

Dsc2 deficiency impairs epithelial–extracellular matrix adhesion

To get further insight into the molecular basis of delayed wound closure in IEC lacking Dsc2 *in vivo*, we utilized the human model IEC

line SKCO15 transfected with short-hairpin RNA (shRNA) for acute KD of Dsc2 versus scramble nonsilencing control (Figure 4A). Epithelial cell monolayers were subjected to scratch-wound healing assays that revealed delayed epithelial wound closure in cells with Dsc2 KD (Figure 4B). Expression of Dsg2 is not perturbed by Dsc2 loss (Figure 4A), suggesting that Dsc2 directly impacts intestinal mucosal wound repair independent of Dsg2. These findings confirm a role of Dsc2 in promoting IEC migration in response to wound injury *in vitro* and corroborate the above *in vivo* findings. In line with our observations, desmosomal proteins (including Dsc2, Dsg2, Dsg3, and Plakophilin-2) have been reported to control cell migration *in vitro* of keratinocytes and cancer cells such as human oral squamous carcinoma cell line or melanoma cells. However, these studies have not revealed consistent results in different cell types and model systems (South *et al.*, 2003; Yin *et al.*, 2005; Todorovic *et al.*, 2010; Fang *et al.*, 2013; Koetsier *et al.*, 2014; Peitsch *et al.*, 2014; Alaei *et al.*, 2016; Rotzer, Hartlieb, *et al.*, 2016; Bendrick *et al.*, 2019). Here, our results show that Dsc2 promotes intestinal epithelial restitution and wound repair.

The importance of mechanical coupling between cells has been documented for diverse multicellular processes, including collective migration during wound healing. Collective migration of epithelial cells during repair requires coordinated modification of cell–cell and cell–matrix adhesive contacts, cytoskeletal restructuring, and cellular protrusions that serve in concert to generate propulsive traction forces (Tambe, Hardin, *et al.*, 2011). To assess the effects of Dsc2 expression on cell adhesive force generation, we used micro-fabricated post array detectors (mPADs) to measure cell-generated forces during cell adhesion to the extracellular matrix. When seeded overnight onto fibronectin-coated mPADs, cells spread and formed multicellular clusters and the data represent a “snapshot” of traction forces in a cell cluster at equilibrium after overnight culture. An image of a cell cluster is outlined in blue and force vectors in green were calculated from post deflections (Figure 4C). The magnitude of traction forces varied across cell clusters with the highest values occurring at the periphery of migrating cell groups. A plot of total traction force represents a sum of the magnitudes of force vectors of each cell cluster periphery. Such analyses have previously been used to map exchange of mechanical forces at cell–cell adhesion sites and to measure strength of forces exchanged between cells across clusters of multiple cells (Ng *et al.*, 2014). We measured post deflections for control and Dsc2 KD cell clusters using SKCO15 cells and detected smaller clusters for Dsc2 KD cells compared with cells expressing Dsc2 (Figure 4C). Furthermore, SKCO15 cell clusters lacking Dsc2 displayed a dramatic defect in traction force generation compared with the control cells. Similarly, KD of Dsc2 in another IEC line, Caco-2BBE revealed a defect in the traction force generation compared with the control cells (Supplemental Figure S2). However, epithelial cell cluster area in control and Dsc2 KD cells were not different (Supplemental Figure S2). Collectively, these findings demonstrate that Dsc2 plays an important

injection and then subjected to DSS-induced colitis by administration of 2.5% DSS for 5 d followed by regular drinking water for 5 d to promote mucosal recovery. Dsc2^{ERAIEC} are more susceptible to colitis and present delayed recovery from colitis, as reflected by (E) significantly greater body weight loss and (F) higher values of DAI, compared with Dsc2^{fl/fl} mice. (E, F) Data are combined values of three independent experiments (30 mice per group) and are expressed as mean ± SEM. Significance is determined by two-way ANOVA. ****p* ≤ 0.001. (G) Representative images of H&E staining of section of Swiss roll mounts of the distal colon of Dsc2^{ERAIEC} mice compared with controls at day 10. Scale bars: 200 μm. (H) Percentage of injury/ulceration that represents the ratio of the length of injured/ulcerated areas (≥50% crypt loss) relative to the entire colon length showing more mucosal ulcerations in Dsc2^{ERAIEC} mice compared with controls. Dots represent individual mice. Data are combined from three independent experiments (14–15 mice per group) and expressed as mean ± SEM. Significance is determined by two-tailed Student's *t* test. ***p* = 0.003.

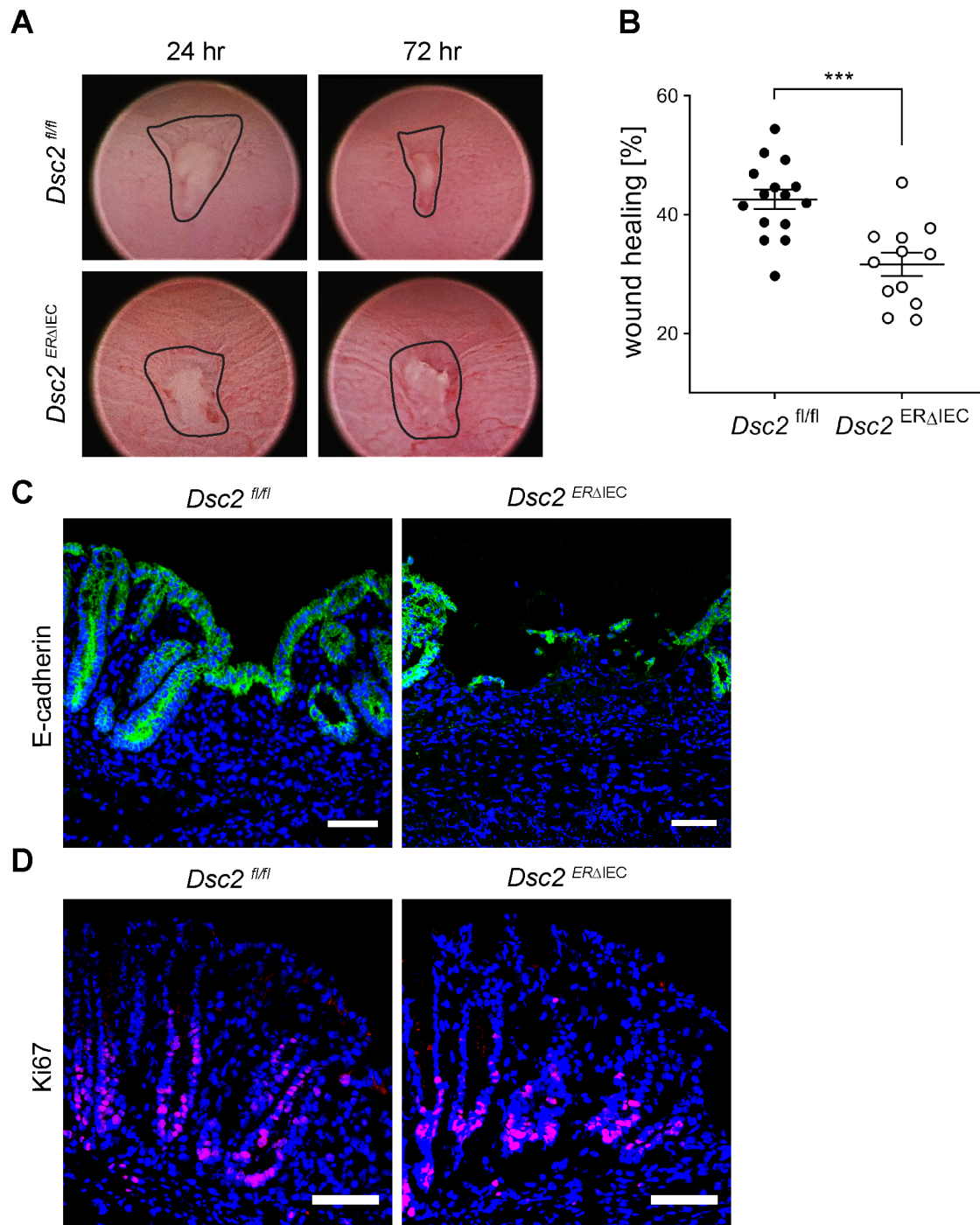


FIGURE 3: Loss of Dsc2 in IEC resulted in impaired colonic mucosal healing after biopsy-induced wound injury. (A) Representative endoscopic images of biopsy-induced colonic wounds at 24 and 72 h postinjury in *Dsc2^{ERΔIEC}* and *Dsc2^{fl/fl}* mice. (B) Digital measurement of wound surface at 24 and 72 h postwounding revealed significant impairment of wound healing in absence of Dsc2 on IEC. Scale bar: 50 μ m. Dots represent the mean value within three to five wounds from individual mice. Data are combined values of two independent experiments with 12–15 mice per group and are expressed as mean \pm SEM. Significance is determined by two-tailed Student's *t* test. ****p* \leq 0.001. (C) IF images of frozen sections of wound beds at 72 h postinjury stained with the epithelial marker E-cadherin (green) and DAPI (blue) showing a dramatic impairment of wound closure in *Dsc2^{ERΔIEC}* mice. *Dsc2^{fl/fl}* mice present a layer of wound-associated epithelial cells that covers the wound that is absent in *Dsc2^{ERΔIEC}* mice. (D) Ki67 staining (magenta) and DAPI counterstain (blue) of frozen sections of crypts immediately adjacent to wound beds at 72 h postinjury revealed similar proliferation rate between *Dsc2^{ERΔIEC}* and *Dsc2^{fl/fl}* mice. C and D show representative IF images of five mice per group. Scale bar: 100 μ m.

role in controlling cell–cell and cell–matrix adhesions and suggest that loss of Dsc2 results in decreased mechanotransduction between IEC and extracellular matrix that leads to impaired down-

stream signaling pathways and impaired IEC migration. In line with our findings, E-cadherin has been reported to influence cell–matrix mechanics that regulate traction stress generation and distribution

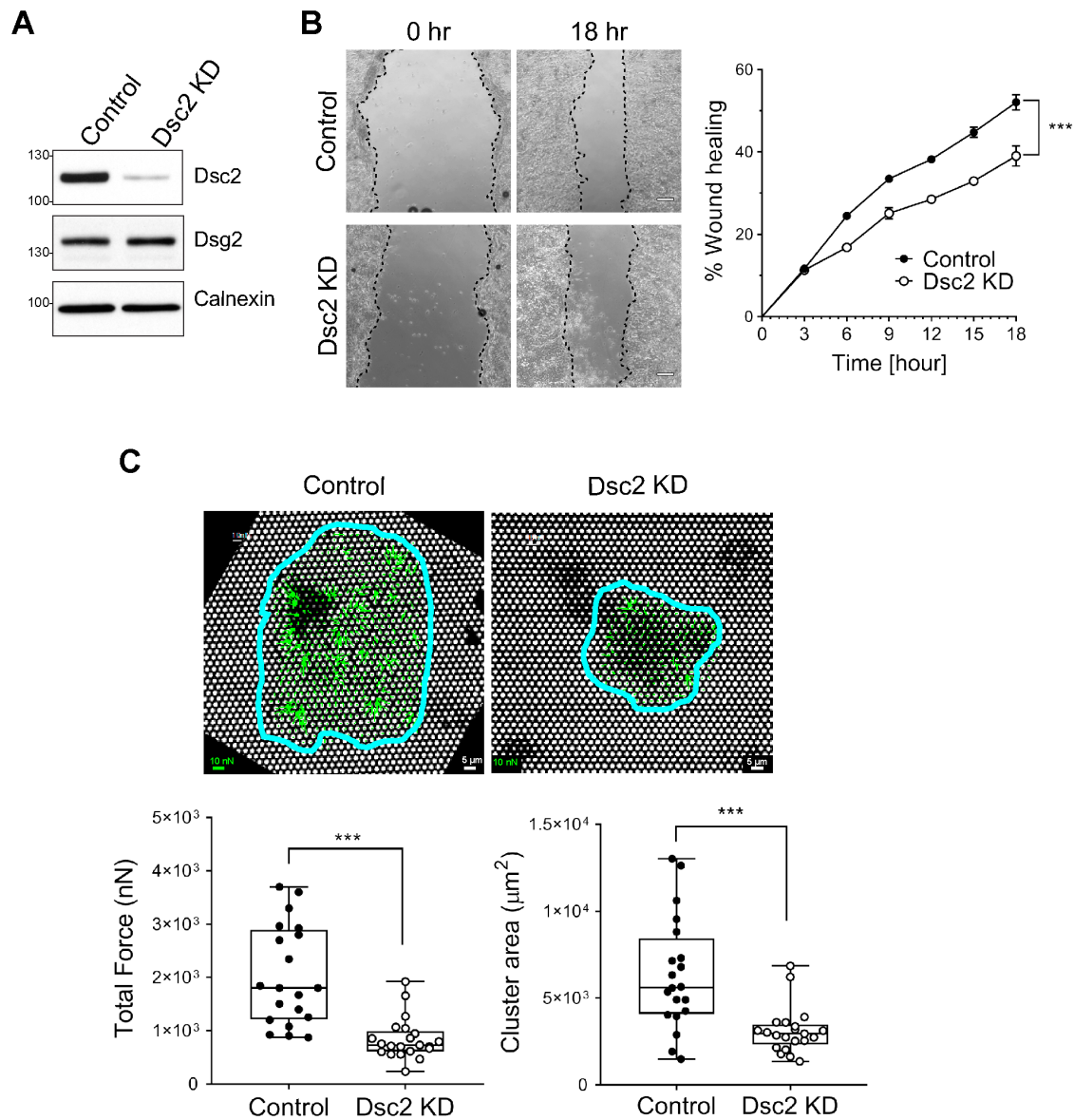
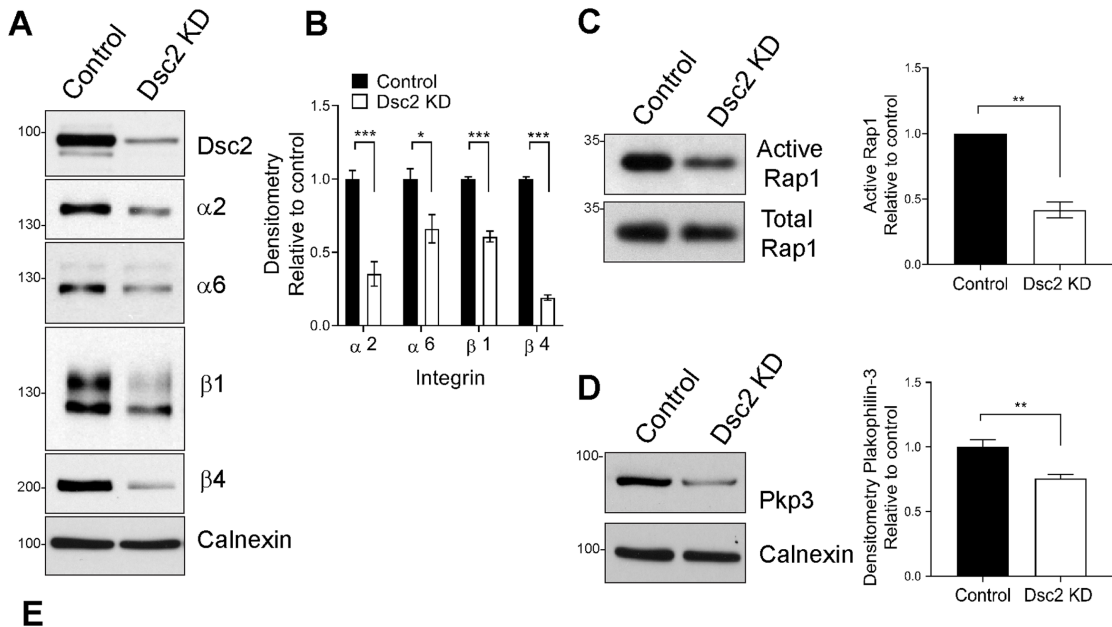


FIGURE 4: Loss of Dsc2 results in impaired wound closure and cell–matrix adhesion in vitro. SKCO15 cells were transduced with Dsc2-specific shRNA (Dsc2 KD) or with a nontargeting shRNA (control). (A) KD of Dsc2 expression was confirmed in SKCO15 by Western blot using anti-Dsc2 antibodies and anti-calnexin as loading control. No major changes were detected in the expression of Dsg2 in the absence of Dsc2. (B) Monolayers of SKCO15 cells were scratch-wounded and monitored for wound closure. Dsc2 KD cells showed significant delayed wound repair compared with control cells. Representative images of wounds at 0 and 18 h. Graph is representative of two independent experiments with three replicates per group and with two independently transduced SKCO15 cell culture. Data are mean \pm SEM. Significance is determined by two-way ANOVA. $***p \leq 0.001$. (C) Measurement of traction forces as well as cluster area within SKCO15 cell KD for Dsc2 (Dsc2 KD) or control cells by using fibronectin-coated microfabricated postarray detectors (mPADs) (see *Materials and Methods*). Representative images show posts (white) with the cell cluster outlined in blue and force vectors (green) calculated from post deflections. Total traction force represents the sum of the magnitudes of the force vectors for each cell cluster. Data consists of 20 cell clusters per condition and are representative of two independent experiments with two independently transduced SKCO15 cell culture. Significance is determined by two-tailed Student's *t* test. $***p \leq 0.001$. Scale bars: 5 μm . Scale for force: 10 nN.

that influences epithelial cell migration (Ng *et al.*, 2012; Mertz *et al.*, 2013). Another desmosomal protein, Plakoglobin, has been reported to play a role in formation of polarized protrusion and keratin cytoskeleton rearrangement after application of force to *Xenopus* mesendoderm cells that results in coordinate changes in cell protrusive behavior required for collective cell migration (Weber *et al.*, 2012).

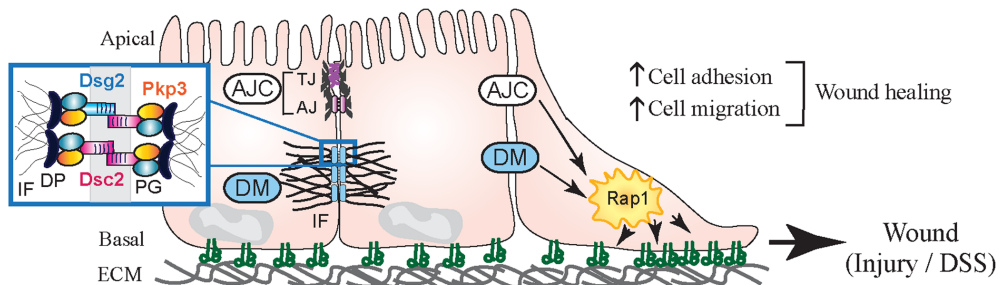
Dsc2 regulates the expression of integrins and Ras-related protein 1 (Rap1) activity

Transmembrane integrin proteins serve as vital regulators and mediators of cell–matrix adhesion and are key players in controlling epithelial cell migration and wound healing (Hynes, 1992; Huttenlocher and Horwitz, 2011; Kenny and Connelly, 2015). Integrins $\alpha 2\beta 1$ (collagen and laminin receptor) and $\alpha 6\beta 4$ (component of



E

Epithelial Dsc2



No epithelial Dsc2

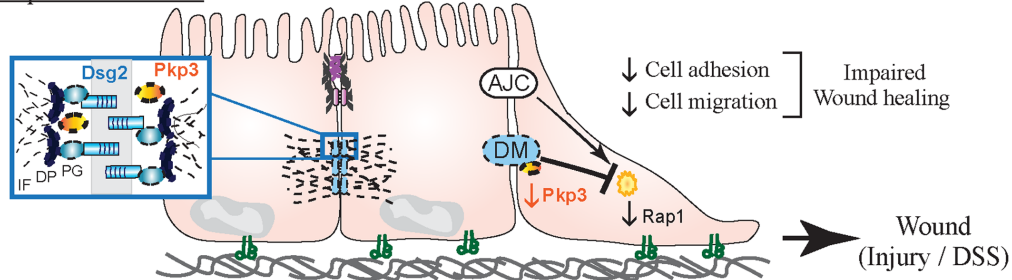


FIGURE 5: Dsc2 controls the expression of integrins, Pkp3 and Rap1 activity in vitro. (A, B) Loss of Dsc2 in SKCO15 cells results in reduced expression of beta 1 and beta 4 integrins. (A) Whole cell lysates from subconfluent monolayer of SKCO15 KD for Dsc2 (Dsc2 KD) or control cells were subjected to SDS-PAGE and immunoblot against Dsc2 and integrin subunits alpha 2, alpha 6, beta 1, and beta 4. Calnexin was used as loading control. Western blot images are representative of four independent experiments. (B) Histograms represent densitometric values normalized to controls from four independent experiments with independently transduced SKCO15 cell culture. Bar graphs are mean \pm SEM. Significance is determined by two-tailed Student's *t* test. $***p \leq 0.001$, $*p = 0.05$. (C, D) Loss of Dsc2 resulted in pull down of less active Rap1 in comparison to control cells. (C) Subconfluent monolayers of SKCO15 KD for Dsc2 (Dsc2 KD) or control cells were subjected to RalGDS pull down followed by SDS-PAGE. GTP-bound Rap1 was detected by Western blotting with anti-Rap1 antibodies. Densitometric quantification of immunoblots of active Rap1 by RalGDS pull down normalized to control. (D) Pkp3 was evaluated in whole cell lysates of SKCO15 KD for Dsc2 (Dsc2 KD) or control cells. Densitometric quantification of immunoblots of Plakophilin 3 normalized to control. (C, D) WB images are representative of three independent experiments with independently transduced SKCO15 cell culture. Bar graphs are mean values from three independent experiments \pm SEM. Significance is determined by two-tailed Student's *t* test. $**p = 0.01$. (E) Model summarizing the role of intestinal epithelial-expressed Dsc2 in mucosal repair after injury. Dsc2 regulates intestinal mucosal wound closure by controlling integrin expression, cell-matrix adhesion dynamics and cell migration. Top panel depicts baseline condition with IEC expressing Dsc2 (red) and Dsg2 (blue) forming mature Desmosome (DM) complexes that promote cell cohesion and contribute to collective migration and wound healing. Signaling pathways downstream of

hemidesmosome and laminin receptor) have been reported by us and others to regulate epithelial wound healing (Lotz *et al.*, 1997; Borradori and Sonnenberg, 1999; Goldfinger *et al.*, 1999; Mercurio *et al.*, 2001; Rankin *et al.*, 2013). We therefore evaluated the effect loss of Dsc2 on expression of these integrins in migrating SKCO15 cells. Immunoblot analysis (WB) revealed that lack of Dsc2 resulted in decreased protein expression of integrin subunits $\alpha 2$, $\alpha 6$, $\beta 1$, and $\beta 4$ (Figure 5, A and B) but not corresponding mRNA (Supplemental Figure S3), implying a posttranscriptional change in integrin proteins after Dsc2 KD. These findings suggested functional interplay between desmosomal cadherins and integrin $\beta 1$ and $\beta 4$. Indeed, it has been reported that Dsg2 can directly interact with integrin $\beta 8$ to promote endothelial cells angiogenesis but there is no evidence of an interaction in IEC (Giusti *et al.*, 2013). Our findings are in line with reports demonstrating a functional interplay between E-cadherin and $\alpha 2\beta 1$ integrin to regulate epithelial cell migration (Borghi *et al.*, 2010; Siret *et al.*, 2015). Furthermore, we have described that other junctional adhesion molecules, such as TJ-associated protein junctional adhesion molecule-A (JAM-A) (Severson *et al.*, 2009) and basolateral membrane protein CD47 (Reed, Luissint, *et al.*, 2019), regulate the expression/stability of integrin $\beta 1$, whereas there is no evidence of direct interaction. Whether Dsc2 interacts physically with integrin $\beta 1$ and $\beta 4$ or regulates stability of these proteins by indirect mechanisms needs further investigation.

To gain further insight into the molecular basis of regulation of cell migration by Dsc2, we investigated the involvement of small GTPases family members that have been reported to regulate cell–matrix interactions, integrin function, and intestinal barrier function (Citalan-Madrid *et al.*, 2013). Surprisingly, among the Rho family of GTPases (including RhoA, Rac1, and Cdc42), we did not observe significant changes in their activity in response to Dsc2 KD in IEC (unpublished data). Therefore, we next determined Rap1 GTPase activity that has been linked to intercellular adhesion molecules and $\beta 1$ integrin activation in epithelial cells (Kinbara *et al.*, 2003). Furthermore, we have previously reported that the complex JAM-A/Rap1 regulates integrin levels in epithelial cells (Mandell *et al.*, 2005) and others have observed that the desmosomal protein Plakophilin-3 (Pkp3) forms a complex with the Rap1 GTPase, promoting its activation and facilitating desmosome assembly and AJ maturation (Hogan *et al.*, 2004; Todorovic *et al.*, 2014). Analysis of Rap1 activation revealed decreased Rap1 activity after Dsc2 KD (Figure 5C). Interestingly, we detected reduced expression of Pkp3 in Dsc2 KD cells in comparison to control cells (Figure 5D), suggesting that Pkp3 may control Rap1 activity, as previously reported in keratinocytes (Todorovic *et al.*, 2014). All together, these findings suggest a signaling axis among Dsc2, Rap1, and integrins $\beta 1$ and $\beta 4$ that orchestrates IEC migration and wound closure (Figure 5E). It is plausible that Dsc2 indirectly controls Rap1 activity through Pkp3. However, we cannot exclude the involvement of other signaling pathways that have been reported to activate Rap1 and promote barrier function such as EPAC (guanine exchange factor [GEF] protein directly activated by cAMP), a main GEF for Rap1 (Todorovic *et al.*, 2014; Ramos *et al.*, 2018).

In conclusion, our findings demonstrate that expression of desmosomal cadherin Dsc2 in IEC regulates intestinal mucosal wound closure. Furthermore, Dsc2 controls transduction of force from the enterocytes to the extracellular matrix through modulation of integ-

rin $\beta 1$ and $\beta 4$ proteins as well as Rap1 activity that orchestrates effective cell migration and wound healing.

MATERIALS AND METHODS

Mice

Mice with selective Dsc2 deficiency in IEC were generated on a C57Bl/6 background by breeding Dsc2 floxed mice (*Dsc2^{fl/fl}*) with mice expressing the inducible mutated estrogen receptor fused to Cre-recombinase under control of the Villin promoter: Villin-Cre^{ERT2}; *Dsc2^{fl/fl}* (*Dsc2^{ERAIEC}*). Mice were bred in-house at the University of Michigan (Ann Arbor, MI) and kept under strict specific pathogen-free conditions with ad libitum normal chow and water. Eight-week-old *Dsc2^{ERAIEC}* and control littermates *Dsc2^{fl/fl}* mice were injected intraperitoneally (i.p.) with 1 mg/100 μ l of tamoxifen (T5648, Sigma) dissolved in sterile corn oil (C8267, Sigma) for 5 consecutive days. Animals were used 4 wk after the last tamoxifen injection. All experiments were approved and conducted in accordance with guidelines set by the University of Michigan Institutional Animal Care and Use Committee.

Cell culture

SKCO15 and Caco-2BBE human model of IEC were grown in high glucose (4.5 g/l) DMEM supplemented with 10% fetal bovine serum, 100 U/ml penicillin, 100 μ g/ml streptomycin, 15 mM HEPES (pH 7.4), 2 mM L-glutamine, and 1% nonessential amino acids on tissue culture-treated plastic as previously described (Ivanov *et al.*, 2007; Kolegraff, Nava, *et al.*, 2011). Knockdown of Dsc2 was established by RNA interference using shRNA targeting Dsc2. Control cells were transduced with a scramble nonsilencing vector (Kolegraff *et al.*, 2011). A shRNA transduction (MOI of 2) of IEC was performed in 60–70% confluent IEC using spinfection method (1200 \times g for 30 min at RT) followed by puromycin selection (1 μ g/ml).

Antibodies and reagents

The following primary monoclonal and polyclonal antibodies were used to detect proteins by IF or WB: mouse anti-human/mouse Dsg-2 (clone AH12.2; WB:1/1000, IF: 1/100) was generated in-house (Nava, Laukoetter, *et al.*, 2007). From Abcam: Ki67 (ab15580; IF:1/250), anti-integrin alpha 2 (ab133557; WB:1/1000), anti-integrin alpha 6 (ab181551; WB:1/1000) and cytokeratin 8 (ab53280; WB:1/40,000), and anti-mouse Pkp3 (ab151401; WB:1/1000). From BD Transduction Laboratories: anti-integrin alpha 4 (Cat. 611233). From Millipore: anti-active Rap1 (Cat. 07-916). From R&D systems: anti-human/mouse E-cadherin (AF748; WB: 1/2000; IF: 1/500), anti-mouse Dsc2 (AF7490; WB:1/500; IF: 1/200), and anti-integrin beta 1 (AF1778; WB: 1/1000). From Sigma: anti-beta actin (A2228; WB:1/5000). From Thermofisher: anti-human Dsc2 (Cat. 326200; WB: 1/1000; IF:1/250).

DSS treatment

Mice were provided with 2.5% wt/vol DSS (40–50 kDa, 14489, Affymetrix) dissolved in the drinking water ad libitum for 5 d followed by 5 d with normal drinking water. Clinical disease assessment was obtained daily, with scores of 0–4 assigned for body weight loss, stool consistency, and presence of blood in stools (Hemocult, Beckman Coulter). The individual scores were added and the average was recorded as the DAI. Higher values of DAI

DM in parallel to those from the AJC activate the small GTPase Rap1 influencing integrin function, thereby promoting cell adhesion to the extracellular matrix (ECM) and cell migration. Bottom panel shows the consequences of Dsc2 absence on IEC that results in reduced expression of Pkp3. Loss of Dsc2 is also associated with reduced cell cohesion, decreased levels of integrin $\beta 1$ and $\beta 4$, and reduced activity of Rap1. AJ, adherens junction; DP, Desmoplakin, IF, intermediate filaments; Integrins are depicted as $\alpha\beta$ complexes; PG, Plakoglobin; TJ, tight junction.

reflect increasing severity of colitis. At the end of the experiment, mice were killed and colon length measured. Hematoxylin-eosin (H&E) staining of sections of Swiss roll mounts of the entire colon (8 μm thick) was performed to quantify colonic mucosal injury (Reed, Luissint, et al., 2019). Percentage of ulceration was calculated as a ratio of the length of injured/ulcerated area ($\geq 50\%$ crypt loss) relative to the entire colon length. Mice were humanely killed before the end of the experiment when weight loss reached more than 20% of the starting body weight, and the Kaplan-Meier method was used to draw the survival curve.

Wound healing assays

For in vitro experiments, Dsc2 shRNA transduced SKCO15 cell monolayers or control cells were cultured on 24-well tissue culture plates to confluency and scratched using a 10 μl pipette tip under suction as we described previously (Babbin et al., 2007). Monolayers were washed to remove cellular debris and medium was changed. Video quantification of scratch-wound closure was performed by imaging wounds at 30-min intervals in an Axiovert Observer live cell microscopy system (Zeiss). Wound closure was quantified at the indicated time points using ImageJ software (National Institutes of Health [NIH]) calculated as percent reduction of cell-free surface area compared with immediately after wounding ($t = 0$).

For in vivo biopsy-based mucosal wound model, a high-resolution video endoscope (Coloview Veterinary Endoscope, Karl Storz) equipped with biopsy forceps was used to create biopsy-induced injury of the colonic mucosa at three to five sites along the dorsal aspect of the colon of anesthetized mice (i.p. injection of ketamine 100 mg/kg, xylazine 5 mg/kg). Wound healing was quantified at 24 and 72 h after injury. Endoscopic procedures were viewed with high-resolution (1024 \times 768 pixels) images on a flat-panel color monitor. Each wound region was photographed at 24 and 72 h, and wound areas calculated using ImageJ. In each experiment, three to five wounds per mouse were quantified (Quiros, Nishio, Neumann, et al., 2017). For IF analysis, wounds were harvested from colons by punch biopsy, embedded, and flash-frozen in OCT embedding compound, followed by sectioning (6 μm thick) and stained as indicated.

IF

Samples of human colonic mucosa from individuals with UC or normal mucosa adjacent to colon cancer resections were collected anonymously under approved human subject guidelines at the University of Michigan. All the patients diagnosed with UC exhibited chronic UC with active inflammation. Frozen tissue sections (6 μm thick) of human samples or mouse colons (untreated or treated with DSS) were fixed at room temperature in 4% paraformaldehyde, followed by blocking and permeabilization with 3% bovine serum albumin (BSA)/0.5% Triton X-100 in phosphate-buffered saline (PBS). Primary antibodies were incubated overnight at 4°C in blocking buffer (3% BSA in PBS), followed by fluorescent secondary antibodies (Invitrogen; 1/500) at room temperature for 1 h. DAPI (4',6-diamidino-2-phenylindole, dihydrochloride) (D1306, Invitrogen) was used to stain nuclei. Slides were washed and mounted with ProLong Antifade Reagent (Thermo Fisher Scientific) prior to analysis as indicated. Fluorescence imaging was performed on a Nikon A1 confocal microscope (Nikon, Tokyo, Japan) in the Microscopy and Image Analysis Laboratory core of the University of Michigan.

Immunoblotting

Western blotting for cell lines and human and mouse colonic tissue homogenates were performed as described previously (Yulis, Quiros,

et al., 2018). Cells were lysed in RIPA buffer (20 mM Tris-base, 150 mM NaCl, 2 mM EDTA, 2 mM EGTA [egtagic acid, calcium chelator], 1% sodium deoxycholate, 1% Triton X-100, 0.1% SDS, pH 7.4) containing protease and phosphatase inhibitor cocktails (Sigma-Aldrich). Whole colon tissue (mouse or human) was homogenized using a homogenizer in RIPA buffer. Protein concentration was determined using the Pierce Protein BCA kit according to manufacturer's protocol. Samples were boiled for 5 min at 100°C in NuPAGE LDS Sample Buffer (Life Technologies; Eugene, OR) with a final concentration of 100 mM dithiothreitol (DTT) (Sigma-Aldrich). Equal quantities of protein samples were loaded into 8% polyacrylamide gels for SDS-PAGE and transferred to polyvinylidene fluoride (PVDF) membrane. Membranes were blocked with either 5% dry milk/Tris-buffered saline (TBS)/0.1% Tween-20 or 3% BSA/TBS/0.1% Tween-20 for phosphorylated proteins, followed by overnight incubation with primary antibodies at 4°C. Membranes were then incubated with appropriate horseradish peroxidase (HRP)-conjugated secondary antibodies for 1 h at room temperature, followed by development using Clarity Western ECL Substrate and image capture by ChemiDoc imager (Bio-Rad).

Traction force measurements

Traction force measurements were performed as previously described (Dumbauld et al., 2013). In brief, elastomeric micropost arrays were fabricated using PDMS replica molding. To make microfabricated post array templates, 1:10 PDMS prepolymer was cast on top of silanized mPAD device silicon masters, cured at 110°C for 30 min, peeled off gently, oxidized with oxygen plasma (Plasma-Preen; Terra Universal), and silanized overnight with (tridecafluoro-1,1,2,2,-tetrahydrooctyl)-1-trichlorosilane (Sigma-Aldrich) vapor under vacuum. To make the final PDMS mPAD device, 1:10 PDMS prepolymer was cast on the template, degassed under vacuum for 20 min, and cured at 110°C for 20 h and gently peeled off the template on a 25-mm-diameter #1 circular coverslip (Electron Microscopy Services). Peeling-induced collapse of the mPADs was rectified by sonication in 100% ethanol, followed by supercritical drying in liquid CO₂ using a critical point dryer (Samdri-PVT-3D; Tousimis). Flat PDMS stamps were generated by casting 1:20 PDMS prepolymer on flat and silanized silicon wafers. Stamps were coated in a saturating concentration of fibronectin (Thermo Fisher) (50 $\mu\text{g}/\text{ml}$ in PBS) and Alexa Fluor 647-labeled fibrinogen (Thermo Fisher) (20 $\mu\text{g}/\text{ml}$ in PBS) for 1 h. These stamps were washed in sterile distilled water and dried under a stream of nitrogen gas. Subsequently, fibronectin-coated stamps were placed in contact with surface-oxidized mPAD substrates (UVO-Model 342; Jelight). mPAD substrates were subsequently transferred to a solution of 0.2% Pluronic F127 (Sigma-Aldrich) for 30 min to prevent nonspecific protein absorption.

SKCO15 or Caco2-BBE cell lines were seeded in growth medium and then allowed to spread overnight. On the next day, mPAD substrates were transferred to a stainless steel coverslip holder (Attoflour Cell Chamber; Invitrogen) for live cell microscopy and placed in a stage top incubator that regulated temperature, humidity, and CO₂ (Live Cell; Pathology Devices). Confocal images were taken with a Nikon C2-Confocal Module connected to a Nikon Eclipse Ti inverted microscope, using a high magnification objective (Plan Achromat 60 \times water immersion VC, N.A. 1.4; Nikon). Post images were captured using a 640-nm laser with a 685/50 filter; the top and bottom of the posts were sequentially imaged. mPAD deflections were analyzed by custom MATLAB code from Jianping Fu's lab (University of Michigan). The resulting force, F , was calculated using Euler-Bernoulli beam theory, in which E , D , L , and δ are the Young's

modulus, post diameter, post height, and post deflection, respectively: $F = \delta (3\pi ED^4)/(64L^3)$.

Rap1 activity assay

Rap1 activity assays were performed according to the manufacturer's instructions (Cell BioLabs, Cat. STA-406-1, San Diego, CA) and as described previously (Fan *et al.*, 2019). Briefly, migrating SKCO15 cells KD for Dsc2 or control cells were lysed in kit-supplied buffer (400 μ l of 25 mM HEPES, pH 7.5, 150 mM NaCl, 1% NP-40, 10 mM MgCl_2 , 1 mM EDTA, 2% glycerol). Cell lysates were incubated with 40 μ l of Ral-GDS agarose beads for 4 h at 4°C to bind active Rap1. The Ral-GDS beads were washed and boiled in 2 \times SDS sample buffer. Entire samples were then analyzed by immunoblot with detection by Rap1 antibody (Millipore; Cat. 07-916, d:1/2000).

Quantitative PCR (qPCR) analysis of integrin expression

RNA samples were prepared from SKCO15 cells (KD for Dsc2 or control cells) using RNeasy kit (QIAGEN). cDNA was synthesized with iScript cDNA synthesis kit (Bio-Rad). RNA levels of integrin beta1, beta 4, alpha 2, and alpha 6 were determined by qPCR using iQ SYBR Green Supermix (Bio-Rad) with various cycles at 95°C for 10 s and 60°C for 30 s on a CFX connect Real-Time System (Bio-Rad). The primers sequence was: GGATTCTCCAGAAGGTG-GTTTCG and TGCCACCAAGTTCCCATCTCC for integrin beta1, GCAGCTTCCAAATCACAGAGG and CCAGATCATCGGACATG-GAGTT for beta 4, GGAACGGGACTTTCGCAT and GGTACTTCG-GCTTTCTCATCA for alpha 2, ATGCACGCGGATCGAGTTT and TTCCTGTTCTGATTAACATGCT for alpha 6, and AATCCCATCAC-CATCTCCA and TGGACTCCACGACGTACTCA for GAPDH. Integrin beta1, beta 4, alpha 2, or alpha 6 to GAPDH relative expression was calculated using the $2^{(-\Delta\Delta C_t)}$ method and the fold change was calculated by comparing the values to those obtained on control.

Statistics

Statistical significance was measured by Student's *t* test; one-way or two-way analysis of variance (ANOVA) using Graphpad Prism software. Significance was set as $p \leq 0.05$. Results are expressed as mean \pm SEM.

ACKNOWLEDGMENTS

We thank the Transgenic and Gene Targeting Core at Emory University, Microscopy and Image Analysis Laboratory, and the Unit for Laboratory Animal Medicine (ULAM) at the University of Michigan Medical School. We additionally thank Roland Hilgarth for technical assistance. This work was supported by the following grants: German Research Foundation Research Fellowship DFG FL 870/1-1 (S.F.) and the People Program (Marie Curie Actions) of the European Union's Seventh Framework Program (FP7/2007-2013) under REA grant agreement No. 608765 (D.H.M.K.), the National Science Foundation Graduate Research Fellowship under Grant No. DGE-1148903 (D.W.Z.), and National Institutes of Health award numbers R01 EB024322 (A.J.G.), DK61739, DK72564, DK79392 (C.A.P.), and R01-DK059888, DK055679, DK089763 (A.N.).

REFERENCES

Boldface names denote co-first authors.

Alaee M, Danesh G, Pasdar M (2016). Plakoglobin reduces the in vitro growth, migration and invasion of ovarian cancer cells expressing N-cadherin and mutant p53. *PLoS One* 11, e0154323.
Babbin BA, Jesaitis AJ, Ivanov AI, Kelly D, Laukoetter M, Nava P, Parkos CA, Nusrat A (2007). Formyl peptide receptor-1 activation enhances intestinal epithelial cell restitution through phosphatidylinositol 3-kinase-dependent activation of Rac1 and Cdc42. *J Immunol* 179, 8112–8121.

Baumgart DC, Sandborn WJ (2012). Crohn's disease. *Lancet* 380, 1590–1605.
Bendrick JL, Eldredge LA, Williams EI, Haight NB, Dubash AD (2019). Desmoplakin harnesses Rho GTPase and p38 mitogen-activated protein kinase signaling to coordinate cellular migration. *J Invest Dermatol* 139, 1227–1236.
Borghi N, Lowndes M, Maruthamuthu V, Gardel ML, Nelson WJ (2010). Regulation of cell motile behavior by crosstalk between cadherin- and integrin-mediated adhesions. *Proc Natl Acad Sci USA* 107, 13324–13329.
Borradori L, Sonnenberg A (1999). Structure and function of hemidesmosomes: more than simple adhesion complexes. *J Invest Dermatol* 112, 411–418.
Brazil JC, Quiros M, Nusrat A, Parkos CA (2019). Innate immune cell-epithelial crosstalk during wound repair. *J Clin Invest* 129, 2983–2993.
Brooke MA, Nitoiu D, Kelsell DP (2012). Cell-cell connectivity: desmosomes and disease. *J Pathol* 226, 158–171.
Bruewer M, Samarin S, Nusrat A (2006). Inflammatory bowel disease and the apical junctional complex. *Ann NY Acad Sci* 1072, 242–252.
Burdett ID, Sullivan KH (2002). Desmosome assembly in MDCK cells: transport of precursors to the cell surface occurs by two phases of vesicular traffic and involves major changes in centrosome and Golgi location during a Ca(2+) shift. *Exp Cell Res* 276, 296–309.
Chidgey M, Dawson C (2007). Desmosomes: a role in cancer? *Br J Cancer* 96, 1783–1787.
Cirillo N, Lanza M, De Rosa A, Cammarota M, La Gatta A, Gombos F, Lanza A (2008). The most widespread desmosomal cadherin, desmoglein 2, is a novel target of caspase 3-mediated apoptotic machinery. *J Cell Biochem* 103, 598–606.
Citalan-Madrid AF, Garcia-Ponce A, Vargas-Robles H, Betanzos A, Schnoor M (2013). Small GTPases of the Ras superfamily regulate intestinal epithelial homeostasis and barrier function via common and unique mechanisms. *Tissue Barriers* 1, e26938.
Dumbauld DW, Lee TT, Singh A, Scrimgeour J, Gersbach CA, Zamir EA, Fu J, Chen CS, Curtis JE, Craig SW, *et al.* (2013). How vinculin regulates force transmission. *Proc Natl Acad Sci USA* 110, 9788–9793.
el Marjou F, Janssen KP, Chang BH, Li M, Hindie V, Chan L, Louvard D, Chambon P, Metzger D, Robine S (2004). Tissue-specific and inducible Cre-mediated recombination in the gut epithelium. *Genesis* 39, 186–193.
Fan S, Weight CM, Luissint AC, Hilgarth RS, Brazil JC, Ettl M, Nusrat A, Parkos CA (2019). Role of JAM-A tyrosine phosphorylation in epithelial barrier dysfunction during intestinal inflammation. *Mol Biol Cell* 30, 566–578.
Fang WK, Liao LD, Li LY, Xie YM, Xu XE, Zhao WJ, Wu JY, Zhu MX, Wu ZY, Du ZP, *et al.* (2013). Down-regulated desmocollin-2 promotes cell aggressiveness through redistributing adherens junctions and activating beta-catenin signalling in oesophageal squamous cell carcinoma. *J Pathol* 231, 257–270.
Farquhar MG, Palade GE (1963). Junctional complexes in various epithelia. *J Cell Biol* 17, 375–412.
Funakoshi S, Ezaki T, Kong J, Guo RJ, Lynch JP (2008). Repression of the desmocollin 2 gene expression in human colon cancer cells is relieved by the homeodomain transcription factors Cdx1 and Cdx2. *Mol Cancer Res* 6, 1478–1490.
Gassler N, Rohr C, Schneider A, Kartenbeck J, Bach A, Obermuller N, Otto HF, Autschbach F (2001). Inflammatory bowel disease is associated with changes of enterocytic junctions. *Am J Physiol Gastrointest Liver Physiol* 281, G216–G228.
Giusti B, Margheri F, Rossi L, Lapini I, Magi A, Serrati S, Chilla A, Laurenzana A, Magnelli L, Calorini L, *et al.* (2013). Desmoglein-2-integrin Beta-8 interaction regulates actin assembly in endothelial cells: deregulation in systemic sclerosis. *PLoS One* 8, e68117.
Goldfinger LE, Hopkinson SB, deHart GW, Collawn S, Couchman JR, Jones JC (1999). The alpha3 laminin subunit, alpha6beta4 and alpha3beta1 integrin coordinately regulate wound healing in cultured epithelial cells and in the skin. *J Cell Sci* 112, 2615–2629.
Gross A, Pack LAP, Schacht GM, Kant S, Ungewiss H, Meir M, Schlegel N, Preisinger C, Boor P, Guldiken N, *et al.* (2018). Desmoglein 2, but not desmocollin 2, protects intestinal epithelia from injury. *Mucosal Immunol* 11, 1630–1639.
Hogan C, Serpente N, Cogram P, Hosking CR, Bialucha CU, Feller SM, Braga VM, Birchmeier W, Fujita Y (2004). Rap1 regulates the formation of E-cadherin-based cell-cell contacts. *Mol Cell Biol* 24, 6690–6700.
Holthofer B, Windoffer R, Troyanovsky S, Leube RE (2007). Structure and function of desmosomes. *Int Rev Cytol* 264, 65–163.
Huber O, Petersen I (2015). 150th Anniversary series: desmosomes and the hallmarks of cancer. *Cell Commun Adhes* 22, 15–28.

- Huttenlocher A, Horwitz AR (2011). Integrins in cell migration. *Cold Spring Harb Perspect Biol* 3, a005074.
- Hynes RO (1992). Integrins: versatility, modulation, and signaling in cell adhesion. *Cell* 69, 11–25.
- Ivanov AI, Bachar M, Babbitt BA, Adelstein RS, Nusrat A, Parkos CA (2007). A unique role for nonmuscle myosin heavy chain IIA in regulation of epithelial apical junctions. *PLoS One* 2, e658.
- Jiang K, Rankin CR, Nava P, Sumagin R, Kamekura R, Stowell SR, Feng M, Parkos CA, Nusrat A** (2014). Galectin-3 regulates desmoglein-2 and intestinal epithelial intercellular adhesion. *J Biol Chem* 289, 10510–10517.
- Kamekura R, Kolegraff KN, Nava P, Hilgarth RS, Feng M, Parkos CA, Nusrat A** (2014). Loss of the desmosomal cadherin desmoglein-2 suppresses colon cancer cell proliferation through EGFR signaling. *Oncogene* 33, 4531–4536.
- Kamekura R, Nava P, Feng M, Quiros M, Nishio H, Weber DA, Parkos CA, Nusrat A (2015). Inflammation-induced desmoglein-2 ectodomain shedding compromises the mucosal barrier. *Mol Biol Cell* 26, 3165–3177.
- Kenny FN, Connelly JT (2015). Integrin-mediated adhesion and mechanosensing in cutaneous wound healing. *Cell Tissue Res* 360, 571–582.
- Kinbara K, Goldfinger LE, Hansen M, Chou FL, Ginsberg MH (2003). Ras GTPases: integrins' friends or foes? *Nat Rev Mol Cell Biol* 4, 767–776.
- Koetsier JL, Amargo EV, Todorovic V, Green KJ, Gotsel LM (2014). Plakophilin 2 affects cell migration by modulating focal adhesion dynamics and integrin protein expression. *J Invest Dermatol* 134, 112–122.
- Kolegraff K, Nava P, Helms MN, Parkos CA, Nusrat A** (2011). Loss of desmocollin-2 confers a tumorigenic phenotype to colonic epithelial cells through activation of Akt/beta-catenin signaling. *Mol Biol Cell* 22, 1121–1134.
- Laukoetter MG, Bruewer M, Nusrat A (2006). Regulation of the intestinal epithelial barrier by the apical junctional complex. *Curr Opin Gastroenterol* 22, 85–89.
- Lotz MM, Nusrat A, Madara JL, Ezzell R, Wewer UM, Mercurio AM (1997). Intestinal epithelial restitution. Involvement of specific laminin isoforms and integrin laminin receptors in wound closure of a transformed model epithelium. *Am J Pathol* 150, 747–760.
- Lowndes M, Rakshit S, Shafraz O, Borghi N, Harmon RM, Green KJ, Sivasankar S, Nelson WJ (2014). Different roles of cadherins in the assembly and structural integrity of the desmosome complex. *J Cell Sci* 127, 2339–2350.
- Luissint AC, Parkos CA, Nusrat A (2016). Inflammation and the intestinal barrier: leukocyte-epithelial cell interactions, cell junction remodeling, and mucosal repair. *Gastroenterology* 151, 616–632.
- Mandell KJ, Babbitt BA, Nusrat A, Parkos CA (2005). Junctional adhesion molecule 1 regulates epithelial cell morphology through effects on beta1 integrins and Rap1 activity. *J Biol Chem* 280, 11665–11674.
- Mercurio AM, Rabinovitz I, Shaw LM (2001). The alpha 6 beta 4 integrin and epithelial cell migration. *Curr Opin Cell Biol* 13, 541–545.
- Mertz AF, Che Y, Banerjee S, Goldstein JM, Rosowski KA, Revilla SF, Niessen CM, Marchetti MC, Dufresne ER, Horsley V (2013). Cadherin-based intercellular adhesions organize epithelial cell-matrix traction forces. *Proc Natl Acad Sci USA* 110, 842–847.
- Najor NA (2018). Desmosomes in human disease. *Annu Rev Pathol* 13, 51–70.
- Nava P, Kamekura R, Nusrat A** (2013). Cleavage of transmembrane junction proteins and their role in regulating epithelial homeostasis. *Tissue Barriers* 1, e24783.
- Nava P, Laukoetter MG, Hopkins AM, Laur O, Gerner-Smidt K, Green KJ, Parkos CA, Nusrat A** (2007). Desmoglein-2: a novel regulator of apoptosis in the intestinal epithelium. *Mol Biol Cell* 18, 4565–4578.
- Nekrasova O, Green KJ (2013). Desmosome assembly and dynamics. *Trends Cell Biol* 23, 537–546.
- Neurath MF (2014). Cytokines in inflammatory bowel disease. *Nat Rev Immunol* 14, 329–342.
- Neurath MF, Travis SP (2012). Mucosal healing in inflammatory bowel diseases: a systematic review. *Gut* 61, 1619–1635.
- Ng MR, Besser A, Brugge JS, Danuser G (2014). Mapping the dynamics of force transduction at cell-cell junctions of epithelial clusters. *Elife* 3, e03282.
- Ng MR, Besser A, Danuser G, Brugge JS (2012). Substrate stiffness regulates cadherin-dependent collective migration through myosin-II contractility. *J Cell Biol* 199, 545–563.
- Nuber UA, Schafer S, Schmidt A, Koch PJ, Franke WW (1995). The widespread human desmocollin Dsc2 and tissue-specific patterns of synthesis of various desmocollin subtypes. *Eur J Cell Biol* 66, 69–74.
- Ordas I, Eckmann L, Talamini M, Baumgart DC, Sandborn WJ (2012). Ulcerative colitis. *Lancet* 380, 1606–1619.
- Papi C, Aratari A (2014). Mucosal healing as a treatment for IBD? *Expert Rev Gastroenterol Hepatol* 8, 457–459.
- Peitsch WK, Doerflinger Y, Fischer-Colbrie R, Huck V, Bauer AT, Utikal J, Goerdts S, Schneider SW (2014). Desmoglein 2 depletion leads to increased migration and upregulation of the chemoattractant secretoneurin in melanoma cells. *PLoS One* 9, e89491.
- Quiros M, Nishio H, Neumann PA, Siuda D, Brazil JC, Azcutia V, Hilgarth R, O'Leary MN, Garcia-Hernandez V, Leoni G, et al.** (2017). Macrophage-derived IL-10 mediates mucosal repair by epithelial WISP-1 signaling. *J Clin Invest* 127, 3510–3520.
- Quiros M, Nusrat A (2019). Contribution of wound-associated cells and mediators in orchestrating gastrointestinal mucosal wound repair. *Annu Rev Physiol* 81, 189–209.
- Ramos CJ, Lin C, Liu X, Antonetti DA (2018). The EPAC-Rap1 pathway prevents and reverses cytokine-induced retinal vascular permeability. *J Biol Chem* 293, 717–730.
- Rankin CR, Hilgarth RS, Leoni G, Kwon M, Den Beste KA, Parkos CA, Nusrat A (2013). Annexin A2 regulates beta1 integrin internalization and intestinal epithelial cell migration. *J Biol Chem* 288, 15229–15239.
- Reed M, Luissint AC, Azcutia V, Fan S, O'Leary MN, Quiros M, Brazil J, Nusrat A, Parkos CA** (2019). Epithelial CD47 is critical for mucosal repair in the murine intestine in vivo. *Nat Commun* 10, 5004.
- Roberts GA, Burdett ID, Pidsley SC, King IA, Magee AI, Buxton RS (1998). Antisense expression of a desmocollin gene in MDCK cells alters desmosome plaque assembly but does not affect desmoglein expression. *Eur J Cell Biol* 76, 192–203.
- Rotzer V, Hartlieb E, Winkler J, Walter E, Schlipf A, Sardy M, Spindler V, Waschke J** (2016). Desmoglein 3-dependent signaling regulates keratinocyte migration and wound healing. *J Invest Dermatol* 136, 301–310.
- Schafer S, Koch PJ, Franke WW (1994). Identification of the ubiquitous human desmoglein, Dsg2, and the expression catalogue of the desmoglein subfamily of desmosomal cadherins. *Exp Cell Res* 211, 391–399.
- Schlegel N, Meir M, Heupel WM, Holthofer B, Leube RE, Waschke J (2010). Desmoglein 2-mediated adhesion is required for intestinal epithelial barrier integrity. *Am J Physiol Gastrointest Liver Physiol* 298, G774–G783.
- Severson EA, Lee WY, Capaldo CT, Nusrat A, Parkos CA (2009). Junctional adhesion molecule A interacts with Afadin and PDZ-GEF2 to activate Rap1A, regulate beta1 integrin levels, and enhance cell migration. *Mol Biol Cell* 20, 1916–1925.
- Siret C, Terziolo C, Dobric A, Habib MC, Germain S, Bonnier R, Lombardo D, Rigot V, Andre F (2015). Interplay between cadherins and alpha-2beta1 integrin differentially regulates melanoma cell invasion. *Br J Cancer* 113, 1445–1453.
- South AP, Wan H, Stone MG, Dopping-Hepenstal PJ, Purkis PE, Marshall JF, Leigh IM, Eady RA, Hart IR, McGrath JA (2003). Lack of plakophilin 1 increases keratinocyte migration and reduces desmosome stability. *J Cell Sci* 116, 3303–3314.
- Spindler V, Meir M, Vigh B, Flemming S, Hutz K, Germer CT, Waschke J, Schlegel N (2015). Loss of Desmoglein 2 contributes to the pathogenesis of Crohn's Disease. *Inflamm Bowel Dis* 21, 2349–2359.
- Syed SE, Trinnaman B, Martin S, Major S, Hutchinson J, Magee AI (2002). Molecular interactions between desmosomal cadherins. *Biochem J* 362, 317–327.
- Tambe DT, Hardin CC, Angelini TE, Rajendran K, Park CY, Serra-Picamal X, Zhou EH, Zaman MH, Butler JP, Weitz DA, et al.** (2011). Collective cell guidance by cooperative intercellular forces. *Nat Mater* 10, 469–475.
- Todorovic V, Desai BV, Patterson MJ, Amargo EV, Dubash AD, Yin T, Jones JC, Green KJ (2010). Plakoglobin regulates cell motility through Rho- and fibronectin-dependent Src signaling. *J Cell Sci* 123, 3576–3586.
- Todorovic V, Koetsier JL, Gotsel LM, Green KJ (2014). Plakophilin 3 mediates Rap1-dependent desmosome assembly and adherens junction maturation. *Mol Biol Cell* 25, 3749–3764.
- Ungewiss H, Vielmuth F, Suzuki ST, Maiser A, Harz H, Leonhardt H, Kugelmann D, Schlegel N, Waschke J (2017). Desmoglein 2 regulates the intestinal epithelial barrier via p38 mitogen-activated protein kinase. *Sci Rep* 7, 6329.
- Waschke J (2008). The desmosome and pemphigus. *Histochem Cell Biol* 130, 21–54.
- Weber GF, Bjerke MA, DeSimone DW (2012). A mechanoresponsive cadherin-keratin complex directs polarized protrusive behavior and collective cell migration. *Dev Cell* 22, 104–115.
- Yin T, Getsios S, Caldelari R, Kowalczyk AP, Muller EJ, Jones JC, Green KJ (2005). Plakoglobin suppresses keratinocyte motility through both cell-cell adhesion-dependent and -independent mechanisms. *Proc Natl Acad Sci USA* 102, 5420–5425.
- Yulis M, Quiros M, Hilgarth R, Parkos CA, Nusrat A** (2018). Intracellular Desmoglein-2 cleavage sensitizes epithelial cells to apoptosis in response to pro-inflammatory cytokines. *Cell Death Dis* 9, 389.